

# Identification of the Switch in Early-to-Late Endosome Transition

Dmitry Poteryaev,<sup>1,3</sup> Sunando Datta,<sup>2,3,4</sup> Karin Ackema,<sup>1</sup> Marino Zerial,<sup>2</sup> and Anne Spang<sup>1,\*</sup>

<sup>1</sup>Biozentrum, University of Basel, Klingelbergstrasse 70, Basel 4056, Switzerland

<sup>2</sup>Max Planck Institute of Molecular Cell Biology and Genetics, Pfotenhauerstrasse 108, Dresden 01307, Germany

<sup>3</sup>These authors contributed equally to this work

<sup>4</sup>Present address: IISER Bhopal, Govindpura, Bhopal, India

\*Correspondence: [anne.spang@unibas.ch](mailto:anne.spang@unibas.ch)

DOI 10.1016/j.cell.2010.03.011

## SUMMARY

Sequential transport from early to late endosomes requires the coordinated activities of the small GTPases Rab5 and Rab7. The transition between early and late endosomes could be mediated either through transport carriers or by Rab conversion, a process in which the loss of Rab5 from an endosome occurs concomitantly to the acquisition of Rab7. We demonstrate that Rab conversion is the mechanism by which proteins pass from early to late endosomes in *Caenorhabditis elegans* coelomocytes. Moreover, we identified SAND-1/Mon1 as the critical switch for Rab conversion in metazoa. SAND-1 serves a dual role in this process. First, it interrupts the positive feedback loop of RAB-5 activation by displacing RABX-5 from endosomal membranes; second, it times the recruitment of RAB-7, probably through interaction with the HOPS complex to the same membranes. SAND-1/Mon1 thus acts as a switch by controlling the localization of RAB-5 and RAB-7 GEFs.

## INTRODUCTION

Material to be taken up by a cell is included into invaginations at the plasma membrane. These invaginations of either tubular or vesicular structure are released from the plasma membrane to the inside of the cell by a fission event. The products of such endocytic events fuse with early endosomes, which are marked by the presence of a small GTPase of the Rab family, Rab5, and by Rab5 effector proteins such as EEA1 and phosphoinositide kinase Vps34. The early endosome is also referred to as the sorting endosome (Spang, 2009), because proteins can be recycled to the plasma membrane, brought to the trans-Golgi network, or targeted for destruction by the lysosome. Lysosomal sorting involves the transfer of proteins to late endosomes, which are equivalent to multivesicular bodies. The late endosomes are marked by another small GTPase of the Rab family, Rab7.

Early endosomes not only fuse with incoming endocytic transport carriers but also undergo homotypic fusion as well as fission

events, as a mechanism whereby recycling cargo is sorted from cargo destined for degradation. In fact, these homotypic fusion events can be considered as a hallmark of early endosomes. The nature of endosomal transport is not resolved. One possibility is that early and late endosomes are rather static entities, between which material is transferred by transport carriers (vesicle transport model). Support for this model has been provided by Vonderheit and Helenius (2005), who observed budding of Rab7 domains from Rab5-positive endosomes. Alternatively, the early endosome could be remodeled to become a late endosome, as in a Rab conversion model. There is a consensus that Rab7 domains are present on early endosomes. Consistent with this possibility, studies have shown that the Rab7 domain grows on the early endosome and converts the Rab5-positive endosome into a Rab7-positive compartment (Rink et al., 2005).

The transition mechanism from early-to-late endosomes is complicated by a positive feedback loop involving Rab5. The recruitment of Rab5 to endosomes by the guanine nucleotide exchange factor (GEF) Rabex5 initiates the subsequent binding and activation of effector molecules such as the phosphoinositide kinase Vps34, which produces PI(3)P. This, in turn, increases the binding of Rab5 and more effector molecules (Christoforidis et al., 1999). While in the vesicle transport model the reinforcement of early endosomal identity poses no problem, the Rab conversion model would predict the requirement for a factor that would disrupt the positive feedback loop to promote the Rab5-to-Rab7 switch (Del Conte-Zerial et al., 2008).

Interestingly, the endocytic machinery is highly conserved from yeast to mammals. Therefore, different experimental systems (e.g., yeast, *Caenorhabditis elegans*, and tissue culture) can be used to address questions about the endocytic core machinery. Macrophage-like *C. elegans* coelomocytes offer the advantage of containing highly active large endosomes, which are easily spotted already at the light-microscope level. The availability of endosomal and lysosomal markers, in combination with the tracing of endocytosed BSA-TR, makes these cells an excellent system to study endocytosis events by life cell imaging in a whole living organism.

In this study, we identified the first important regulator, SAND-1/Mon1, in the Rab conversion process. We demonstrate that SAND-1/Mon1 acts as a disruptor of the positive feedback loop by displacing RABX-5 from early endosomal membranes.

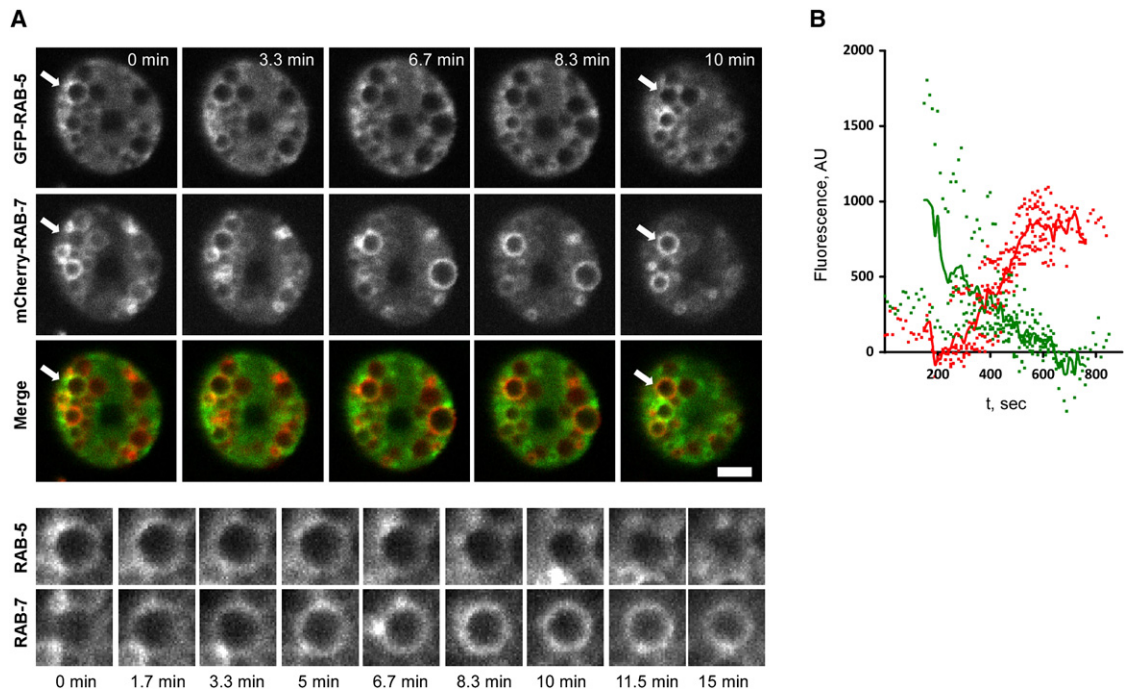


**Figure 1. Endocytic Rab Conversion in *C. elegans* Coelomocytes**

(A) Live-cell imaging of coelomocytes expressing GFP::RAB-5 and mCherry::RAB-7. The arrow points toward the endosome undergoing RAB-5 to RAB-7 conversion. The lower panel shows the magnification of the same endosome.

(B) Quantification of RAB-5 and RAB-7 signals, based on five independent recordings. The lines represent averaged signals; the dots show individual values in fluorescence arbitrary units.

See also Figure S1 and Movie S2.

Moreover, SAND-1/Mon1 actively drives the recruitment of Rab7 onto endosomes, most likely through interaction with the Rab7 guanine exchange factor complex HOPS. Therefore, we propose that SAND-1/Mon1 is the switch in early-to-late endosome maturation (Rab conversion) that regulates the activity state of Rab5 and Rab7.

## RESULTS

### RAB-5 Accumulates on Large Early Endosomes in *sand-1(or552)* Coelomocytes

Previously, we have shown that SAND-1 plays a crucial role in the recruitment of RAB-7 to endosomal membranes in oocytes and in coelomocytes in *C. elegans* (Poteryaev et al., 2007). Moreover, we observed that loss of SAND-1 function results in a large accumulation of RAB-5 protein, as measured by immunoblotting lysate from *sand-1(or552)* worms (Poteryaev et al., 2007). We now find that most of this additional RAB-5 is associated with early endosomes that are still able to undergo homotypic membrane fusion (see Figure S1A and Movie S1 available online). The block of the transition from early to late endosomes and the continued activation of RAB-5 is a likely explanation for the enlarged endosomes found in *sand-1(or552)* animals. This phenotype is reminiscent of the phenotype observed after overexpression of the dominant-active form of Rab5 in mammalian cells (Rink et al., 2005; Rosenfeld et al., 2001; Stenmark

et al., 1994) (Figures S3A–S3D) or overexpression of the yeast Rab5, Ypt51a/Vps21, in yeast (Gerrard et al., 2000). Together, these observations suggest that, in the absence of SAND-1, RAB-5 retained on the endosomal membrane is at least partially in the active state and that the positive feedback loop initiated by RAB-5 is still active. Therefore, SAND-1 could play two roles in early-to-late endosome transport: first, SAND-1 might be required for the repression of RAB-5 on early endosomes, and second, it might play a direct role in the recruitment and/or activation of RAB-7 on these endosomes.

### Rab Conversion Takes Place on Endosomes in *C. elegans* Coelomocytes

So far, Rab conversion has been demonstrated in only one mammalian cell line (Rink et al., 2005). To establish that Rab conversion is a more general and widely used mechanism and that SAND-1 is potentially involved in this process, we expressed GFP::RAB-5 and mCherry::RAB-7 in coelomocytes and monitored the disappearance of GFP::RAB-5 and the acquisition of mCherry::RAB-7 on the same endosomes over time (Figure 1). Coelomocytes are especially well suited for this kind of experiment, because their endosomes are unusually large, and they appear in the light microscope as spheres with a lumen and a limiting membrane. The expression of the exogenous proteins in coelomocytes did not alter the size or distribution of endosomes, compared with coelomocytes that did not express any

marker and in which the endocytic pathway was highlighted by uptake of the fluid-phase marker BSA-Texas Red (BSA-TR) or secreted soluble GFP (Poteryaev et al., 2007). When we imaged coelomocytes expressing both GFP::RAB-5 and mCherry::RAB-7 using 4D-microscopy, we observed that early endosomes lost the GFP::RAB-5 signal over time and synchronously acquired mCherry::RAB-7 (Figure 1A, arrows point to an endosome undergoing conversion, Movie S2). We cannot exclude that small vesicles could also form but these are not detectable by this method and do not appear to have a major contribution in early-to-late endosomes transition. Quantification of the fluorescent signal revealed that the kinetics of RAB-5 depletion and RAB-7 recruitment to the same endosomal membrane were similar to one another (Figure 1B). These data demonstrate that Rab conversion is a general mechanism for early-to-late endosome transport and support the idea that this mechanism is conserved throughout metazoa.

### SAND-1 Interacts with the Guanine Nucleotide Exchange Factor of RAB-5, RABX-5

If SAND-1 were required for terminating the positive feedback loop of RAB-5 activation, one might expect that SAND-1 should block RAB-5 activation in some way. Because the SAND-1 did not bind RAB-5 by yeast two-hybrid assay, and the mammalian homolog Mon1 did not interact with the inactive or active form of Rab5 in vitro (Figure S2A), we tested the interaction of SAND-1 with RAB-5 GEFs, which are all VPS9 domain-containing proteins. Three VPS9 domain-containing proteins have been annotated in the *C. elegans* genome: RABX-5, RME-6, and TAG-333. RME-6 is supposed to function at the onset of endocytosis at the plasma membrane and has partially overlapping function with RABX-5 (Sato et al., 2005). The function of TAG-333 remains elusive, but it cannot substitute for either RABX-5 or RME-6. We found that SAND-1 interacted specifically with RABX-5 in a yeast two-hybrid assay (Figure 2A and Figure S2C), and that His<sub>6</sub>-RABX-5 bound to GST-SAND-1 (Figure S2B). Moreover, recombinant Mon1a and Mon1b interacted with GST-Rabex5 in vitro (Figure S2E and Figure 2B). We mapped the interaction site of SAND-1 to the helical bundle of RABX-5 (Figure 2A and Figure S2D). Interestingly, the helical bundle serves a dual purpose: it stabilizes the VPS9 domain and contributes to the GEF activity (Delprato et al., 2004). In addition, the helical bundle together with the upstream helix constitutes the early-endosome-targeting domain (Zhu et al., 2007). We first tested whether the mammalian ortholog of SAND-1, Mon1b, could influence the guanine nucleotide exchange activity of Rabex-5 in vitro. However, we could not detect any major changes in the exchange rates on Rab5 using a fluorescent read-out assay (Figure S2F). Moreover, Rabex-5 did not exchange guanine nucleotide on Rab7 independently of the presence of Mon1b (Figure S2F). Finally, RABX-5 seems to act upstream of SAND-1, because *rabex-5(RNAi)* rescued the large endosome phenotype of the *sand-1(or552)* mutant (Figure S1B) similarly to the knockdown of RAB-5, clathrin heavy chain (Poteryaev et al., 2007) or the plasma membrane RAB-5 GEF RME-6 (Figure S1B). Therefore, it seems unlikely that the main function of SAND-1 is to interfere with the catalytic activity of RABX-5.

### RABX-5 Is Trapped on Early Endosomes in the *sand-1(or552)* Mutant

Because SAND-1 had no significant impact on RABX-5 GEF activity, we next tested whether SAND-1 interferes with RABX-5 localization. First, we demonstrated that GFP::RABX-5 is localized to early endosomes in coelomocytes by following the endocytic marker BSA-TR (Figure 2C and Figures S2G and S2H). RABX-5 was not continuously present on a particular endosome but was released within a time frame of 1–2 min (Figure 2C and Figures S2G and S2H). However, the enlarged endosomes in *sand-1(or552)* remained RABX-5 positive even after a 60 min chase period of BSA-TR, whereas in wild-type coelomocytes, all BSA-TR is found in lysosomes after a 60 min chase (Poteryaev et al., 2007). Moreover, the fluorescence intensity ratio of GFP::RABX-5 between the cytoplasm and endosomes was strongly increased in *sand-1(or552)* compared to wild-type coelomocytes (Figure 2E). These data demonstrate that, in the absence of SAND-1 function, RABX-5 is trapped on the early endosome. Furthermore, these results suggest that under these conditions more RAB-5 is activated and the positive feedback loop is not interrupted. Therefore, the conversion to the late endosome cannot occur.

### Knockdown of Mon1a/b Causes Large Early Endosomes to Accumulate in Mammalian Cells

Next we asked whether the role of SAND-1 in Rab conversion is conserved throughout metazoa. SAND-1 has two homologs in vertebrates, Mon1a and Mon1b, neither of which has been implicated in early-to-late endosome transport. HeLa cells expressing GFP-tagged Rab5c under the endogenous promoter were transfected with siRNAs specifically silencing either the Mon1a or Mon1b or both and quantified the effects on the size of the fluorescently labeled early endosomes using MotionTracking software (Rink et al., 2005). The efficiency of the knockdowns was quantified by qRT-PCR and immunoblot (Figures 3A and 3B). Although individual knockdown of Mon1a or Mon1b affected only mildly early endosome morphology (data not shown), the double knockdown caused GFP-Rab5c-positive endosomes to be strongly enlarged (Figure 3C). These enlarged Rabex-5-positive endosomes were still competent in the uptake of Dil-LDL (Figure 3D), similar to the phenotype observed in *C. elegans*. These results suggest that the concomitant depletion of both Mon1a and Mon1b causes the accumulation of Rab5 on expanded endosomes similar to the expression of the activated Rab5 mutant, arguing that Rab conversion is impaired and, thus, that the function of SAND-1 is conserved throughout metazoa.

### Mon1a/b Displace RABX5 from Endosomal Membranes

RABX-5 is trapped on early endosomes in the absence of functional SAND-1 (Figure 2). If this entrapment were a direct consequence of loss of SAND-1 function, overexpression of SAND-1 would be sufficient to remove RABX-5 from endosomes. To test this possibility, we overexpressed Mon1a/b in HeLa cells expressing GFP-Rabex5 (Figure 4). This overexpression caused the redistribution of Rabex5 from endosomes to smaller vesicles, which are likely of endocytic origin (Figures 4B–4E and 4G). Interestingly, a subpopulation of Mon1a/b colocalized with Rabex5 on some endosomal structures. Moreover,

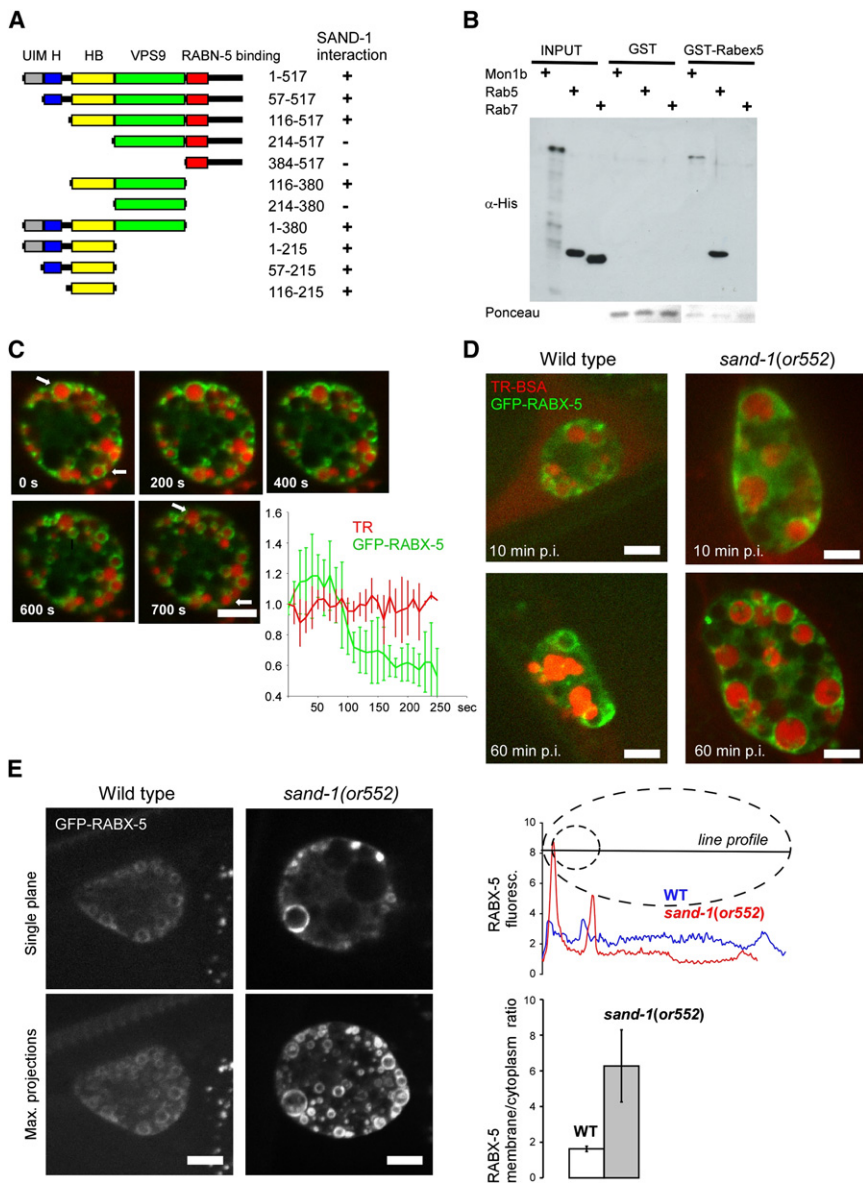


**Figure 2. SAND-1 Interacts with the RAB-5 GEF, RABX-5**

(A) Schematic drawing depicting the SAND-1 interaction with the helical bundle domain of RABX-5 in yeast two-hybrid assay.

(B) The mammalian SAND-1 homolog Mon1b interacts with Rabex5 in vitro. GST pull-down with either immobilized GST or GST-Rabex5 and incubated with His<sub>6</sub>-Mon1b, His<sub>6</sub>-Rab5, or His<sub>6</sub>-Rab7. The bound proteins were detected with antibodies against the His-tag. In the input lanes, 10% of the protein present in the assay were loaded. The amount of immobilized GST and GST-Rabex5 was determined by staining the membrane after transfer with Ponceau.

(C) Live imaging of GFP::RABX-5 (in green) in wild-type *C. elegans* coelomocytes. The early endosomes are filled with the endocytic tracer BSA-TR (red), which was injected into the body cavity 15 min before image collection. The arrow points to the endosome, which gradually lost RABX-5 from its membrane. The graph shows the averaging of five independent recording of RABX-5 and TR signals. Error bars represent standard deviation.

(D) In *sand-1(or552)* mutants, the endosomes remained RABX-5 positive and retained TR even after extended chase periods. In the wild-type, BSA-TR rapidly exits RABX-5 positive compartment.

(E) The endosome-to-cytoplasm ratio of RABX-5 is strongly increased in *sand-1(or552)* mutants. The exposure time is the same for the confocal images. Typical line profile measurement across coelomocytes in wild-type and *sand-1(or552)* mutants are shown. The dotted contours schematically represent the cell boundary and individual RABX-5 positive endosomes. Average RABX-5 membrane-to-cytoplasm ratio based on 54 line profiles from eight individual coelomocytes is shown. The size bars in (C–E) represent 5  $\mu$ m. See also Figure S2.

the soluble pool of Rabex5 was significantly increased (Figure 4F). Thus, Mon1a/b overexpression affects GFP-Rabex5 localization in HeLa cells. To gain more mechanistic insights about the effects of SAND-1/Mon1 on Rabex5, we incubated enriched endosomal fractions with recombinant Mon1b and subjected the mixture to buoyant density centrifugation, which caused the membranes to float and soluble proteins to be retained in lower fractions. The addition of Mon1b caused the relocation of at least a part of Rabex5 from the membrane-bound to the soluble pool of proteins (Figure 4H). As a consequence of the dissociation of Rabex5 from the endosomes, Rab5 association with endosomes should be impaired. Indeed, the cumulative size of Rab5-positive structures decreased upon Mon1a/b overexpression, indicating that the soluble Rab5 pool was increased (Figures S3E–S3J). This effect was specific because the dominant-active form of Rab5 would not

redistribute (Figures S3K–S3P). In fact, overexpression of the dominant-active form of Rab5 caused a massive increase in the size of early endosomes (Figures S3A–S3D), as had been observed elsewhere (Seachrist et al., 2000). These data strongly suggest that SAND-1/Mon1 regulate Rabex5 by displacing it from endosomes.

#### SAND-1 Displaces RABEX-5 from Yeast Endosomes

To corroborate these results, we turned to *Saccharomyces cerevisiae* as a model system. The endocytic pathway is well conserved between yeast and metazoan, and overexpression of a protein is easier to achieve and to control in yeast than in *C. elegans*. Therefore, we expressed *C. elegans* GFP::RABX-5 under the inducible *MET25* promoter (the lower the methionine concentration, the higher the gene expression) in wild-type yeast cells. GFP-RABX-5 was found on endosomes (Figure 5A), as

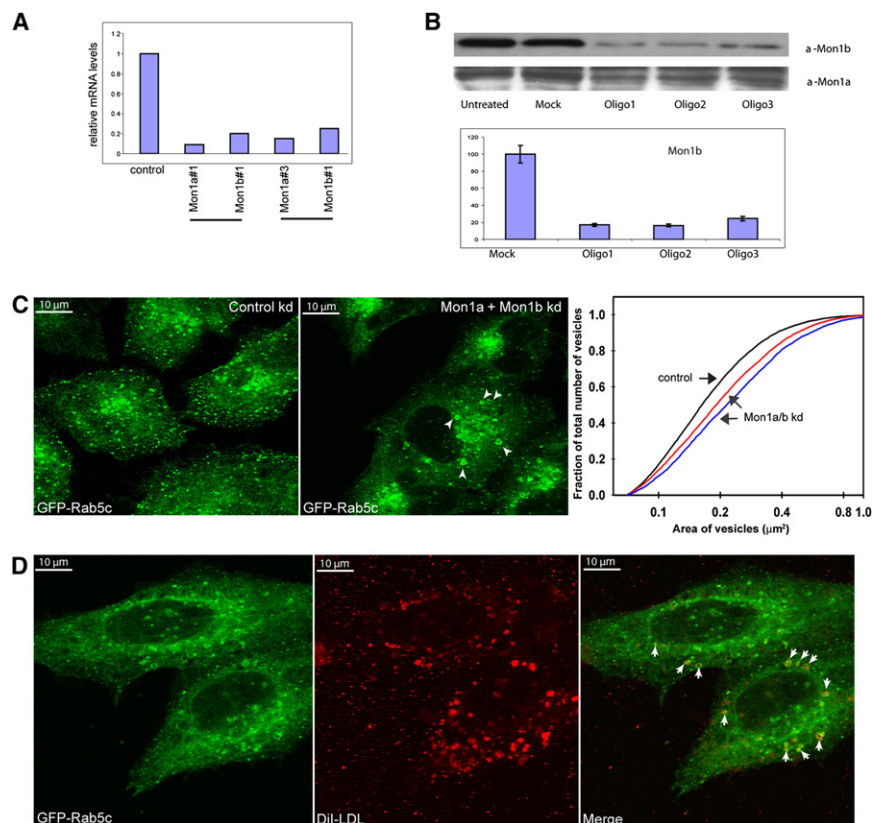


### Figure 3. Knockdown of Mammalian Mon1a/b in Bac-GFP-Rab5c HeLa Cells Results in Enlarged Early Endosomes

(A) Quantification of the mRNA levels of Mon1a and Mon1b after knockdown. Quantitative real-time PCR was performed on samples from 72 hr after transfection. Shown are relative mRNA levels of Mon1a and Mon1b of cells transfected with either a control siRNA or different oligos targeting Mon1a and Mon1b. The mean of 3 independent experiments is shown.

(B) Immunoblot verifying the knockdown of Mon1a and Mon1b. Quantification of the three independent Mon1b blots revealed a similar reduction of the protein level by three different oligos. Error bars represent standard deviations.

(C) Bac-GFP-Rab5c HeLa cells in which Mon1a and Mon1b were knocked down, were fixed 72 hr after transfection and imaged. The area of GFP-Rab5c-positive vesicles was calculated using the Motion tracking software. The cumulative distribution of areas of GFP-Rab5c endosomes/vesicles from the control (black line) and two independent Mon1a/b knockdown conditions (red and blue lines) are shown.

(D) Enlarged GFP-Rab5c positive structures after Mon1a/b knockdown are early endosomes. Cells were treated as in (C), except that after 72 hr after transfection, the cells were incubated with DiI-LDL for 30 min prior to fixation.

indicated by staining endosomes with FM4-64 (Figure 5A and Figure S4). Furthermore, strong overexpression of RABX-5 stimulated homotypic endosome fusion in yeast (Figure 5A, 1x Met, empty vector). This phenotype is very similar to the one observed after overexpression of the endogenous yeast Rab5, Ypt51a/Vps21 (Gerrard et al., 2000). The homotypic endosome fusion was dependent on RABX-5 expression because down-regulating its expression (by the increasing methionine levels in the medium) reduced the size of the endosomes (Figure 5A, 2x Met). We conclude that *C. elegans* RABX-5 is functional in yeast and that it can activate Ypt51a/Vps21 in yeast.

Next, we coexpressed GFP-RABX-5 and SAND-1 from a constitutive promoter (Figure 5A, GPD-sand-1) in the same cells. GFP-RABX-5 changed its localization from endosomal to cytoplasmic. To verify that the effect is indeed due to the expression of SAND-1, we expressed SAND-1 under the control of the ADH promoter, which retains only about 10% of its activity when cells are grown on nonfermentable carbon sources such as EtOH or glycerol. In the presence of nonfermentable carbon sources, RABX-5 was found on endosomes (Figure 5B). Switching the growth medium to a fermentable carbon source (glucose) shifted RABX-5 localization to the cytoplasm. In addition, we expressed a SAND-1 construct that only contains the N-terminal longin domain of SAND-1 and is even shorter than the initially identified genetic lesion in *C. elegans*. The expression of the longin domain of SAND-1 had no effect on RABX-5 association with early endosomes (Figure 5B). Finally, we expressed only the VPS9 domain of RABX-5 (Figure 5C;

GFP-RABX-5<sub>214-380</sub>), which did not interact with SAND-1 (Figure 2A) in yeast. GFP-RABX-5<sub>214-380</sub> was localized to endosomes independently of the presence of SAND-1 (Figure 5C). These data are in agreement with the *C. elegans* phenotype where, in the absence of SAND-1, early endosomes are greatly enlarged (Poteryaev et al., 2007). Moreover, as RABX-5 levels decreased on early endosomes in coelomocytes, SAND-1 levels also increased on the same endosome (Figures S4C and S4D). We conclude that SAND-1 causes the dissociation of RABX-5 from endosomes, supporting the hypothesis that SAND-1 regulates Rab conversion.

Similar to the effect observed in HeLa cells (Figure 4), overexpression of SAND-1 not only reduced the size but also increased the number of early endosomal structures marked by GFP-RAB-5, because homotypic endosome fusion was turned off prematurely (Figure 5D). These results support the argument that SAND-1 acts by blocking the RAB-5-positive feedback loop, thereby driving Rab5-to-Rab7 conversion.

### SAND-1 May Sense the Size of Endosomes, PI(3)P Levels, or a Combination of Both to Bind to Mature Early Endosomes

SAND-1 is mostly cytoplasmic, and only a fraction of the protein is associated with membranes (Poteryaev et al., 2007). How does SAND-1 sense when to localize to the early endosomes in order to displace RABX-5 and block the positive feedback loop? This cannot be accomplished by the recognition of RABX-5 alone because if so, early endosomes would not be

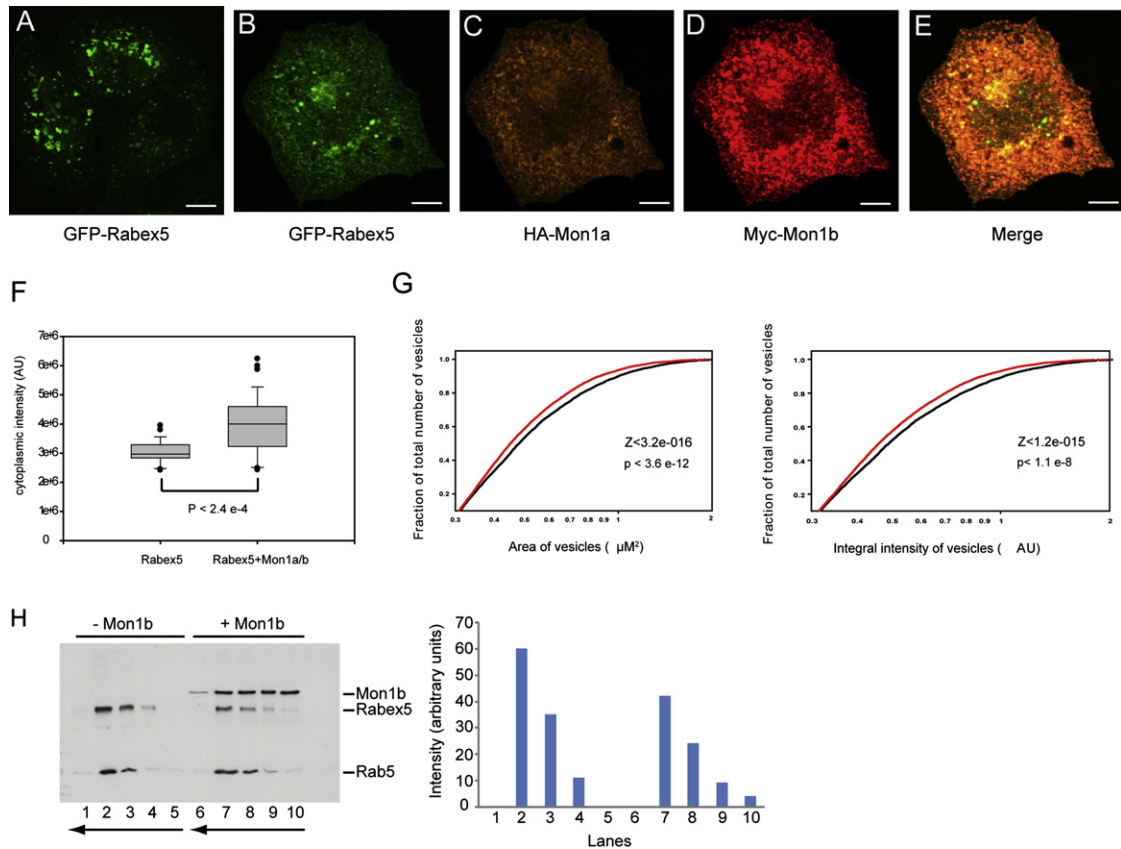


**Figure 4. Mon1a/b Displace Rabex5 from Endosomes In Vivo and In Vitro**

(A–E) GFP-Rabex5 alone (A) was transfected into HeLa cells or cotransfected with HA-Mon1a and Myc-Mon1b (B–E). Cells were fixed 24 hr after transfection and stained with  $\alpha$ -HA and  $\alpha$ -Myc antibody.

(F) Mon1a/b overexpression causes Rabex5 to dissociate from early endosomes. The cytoplasmic Rabex5-GFP staining was quantified in cells expressing Mon1a/b and compared to the staining in control cells. Areas and total intensities of the cytoplasmic Rabex5 signal increased significantly in cells coexpressing Mon1a/b.

(G) The areas and the total intensities of GFP-Rabex5-positive vesicles were measured using the Motion tracking software. The cumulative distributions of areas and total intensities of GFP-Rabex5 vesicles have been plotted. In both panels, the black curve represents the data from the cells expressing only GFP-Rabex5, whereas the red curve represents the data from the cells coexpressing GFP-Rabex5, HA-Mon1a, and Myc-Mon1b. A Z test has been performed indicating the statistical significance. The scale bars represent 10  $\mu\text{m}$ .

(H) Recombinant Mon1b displaces Rabex5 from endosomes in vitro. Purified endosomes from HeLa cells were incubated with recombinant Rabex5-Rabaptin5 and Rab5-GDI. The endosomes were reisolated and unbound Rabex5-Rabaptin5 and Rab5-GDI were removed. To one half of endosomes, Mon1b was added. After the incubation, endosomes were floated on a Histodenz gradient. The fractions were collected from the top, and the Rabex5 and Rab5 distribution was monitored. The second fraction from the top contains the intact endosomes. The arrows indicate the movement of the endosomes in the gradient. The two bottom fractions contain soluble proteins.

See also Figure S3.

able to undergo homotypic fusion and thus mature prior to becoming late endosomes. Because early endosomes undergo homotypic membrane fusion and, hence, must increase in size, we wondered whether early endosomes would turn over into late endosomes only after reaching a critical size. Interestingly, early endosomes would undergo conversion in *C. elegans* coelomocytes after reaching about 2.3  $\mu\text{m}$  in diameter, and endosomes acquiring SAND-1 would be about the same size (Figure 6A). Therefore, the size or the age of the early endosome could be one determinant to recruit SAND-1. One of the key effectors of Rab5 on early endosomes is the type III PI(3)-kinase, Vps34 (Shin et al., 2005), which produces PI(3)P, the hallmark lipid on early endosomes (Gillooly et al., 2000). Thus the “older”

the early endosome, the higher the PI(3)P levels might be. Hence, SAND-1 may recognize PI(3)P on membranes. To test this possibility, we assayed for the ability of recombinant SAND-1 to bind to phospholipids using a protein-lipid overlay assay. SAND-1 recognized monophosphorylated phosphoinositides, most strongly PI(3)P (Figure 6C). The PI(3)P recognition site is most likely contained within the first 333 amino acids, whereby the first 266 amino acids seem to be more important for phospholipid binding (Figure S5). Moreover, when we treated worms with the PI(3)P kinase inhibitor wortmannin, SAND-1 was no longer enriched on endosomes (Figures 6B and 6D). This treatment did not affect the association of RABX-5 with early or RAB-7 with late endosomes, both of which bind independently of

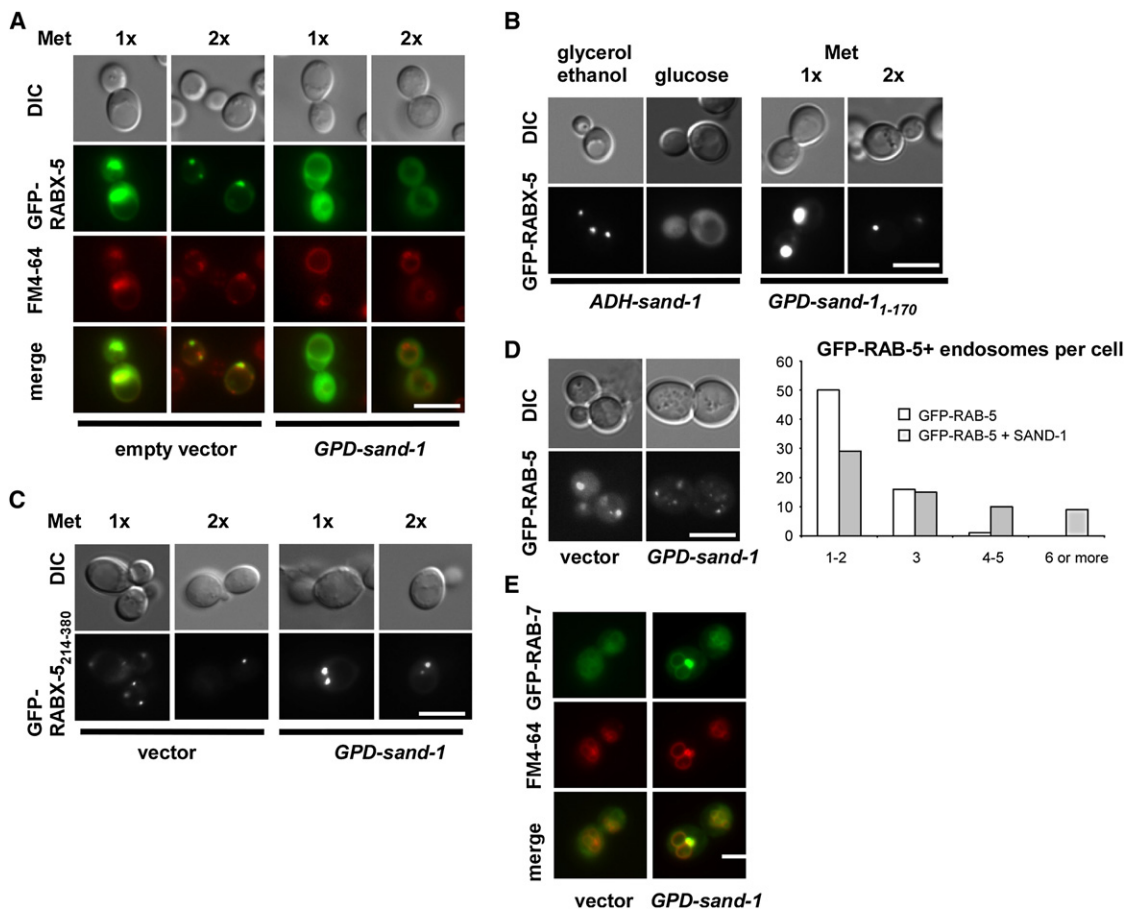


### Figure 5. SAND-1 Displaces RABX-5 from Yeast Endosomal Membranes

(A) The effect of SAND-1 expression on the localization of GFP-RABX-5 in yeast cells. GFP-RABX-5 expression was regulated by methionine levels. 1x refers to the standard concentration of methionine in HC medium (20 mg/l); 2x is 40 mg/l. GPD-sand-1 indicate the panel in which *C. elegans* SAND-1 was expressed from the yeast GPD promoter. FM4-64 staining was used to visualize endosomes and vacuoles.

(B) Strongly reduced levels of SAND-1 expression caused GFP::RABX-5 to remain on the endosomal membranes (left panel) Truncated SAND-1 is unable to displace GFP-RABX-5 from the endosomal membranes (right panel).

(C) The VPS9 domain of RABX-5 is sufficient to associate with endosomes. SAND-1 coexpression had no effect on its localization.

(D) SAND-1 coexpression reduces the size and increases the number of GFP::RAB-5-positive endosomes in yeast. In the graph, the y-axis represents the number of cell scored for each category basket.

(E) *C. elegans* RAB-7 requires SAND-1 for vacuole and late endosome localization. GFP-RAB-7 was expressed in yeast cells in which SAND-1 was expressed from the GPD promoter or in which a vector control was present. The vacuole was visualized by FM4-64. The bar represents 5  $\mu$ m in each of the panels.

See also Figure S4.

PI(3)P to endosomes (Figure 6B). Therefore, SAND-1 would bind specifically to PI(3)P-containing endosomes. Whether the interaction of SAND-1 with PI(3)P alone is sufficient for the recruitment to endosomes remains to be determined. The affinity of SAND-1 for PI(3)P is not very high because SAND-1 could not be floated with PI(3)P-containing liposomes in a buoyant density gradient (data not shown).

### SAND-1 and RAB-7 Arrive Concomitantly on Mature Early Endosomes

We have shown so far that SAND-1 disrupts the RAB-5-positive feedback loop by displacing RABX-5 from endosomes. The next question is whether SAND-1 plays also a direct role in the recruitment of RAB-7 to endosomes. If so, then RAB-7 should never

localize to endosomes prior to membrane recruitment of SAND-1. To test this prediction, we first imaged the arrival of SAND-1 on endosomes in comparison to the recruitment of RAB-7 (Figure 7 and Movie S3). As predicted, RAB-7 never preceded SAND-1 arrival on endosomes. Rather, they always arrived concomitantly. Moreover, although the levels of RAB-7 continued to rise over time, SAND-1 persisted on the endosomes only for 2–3 min before disappearing. We have shown previously that, in *sand-1* mutants, RAB-7 is no longer recruited to endosomes (Poteryaev et al., 2007). Conversely, one would expect that SAND-1 actively supports the recruitment of RAB-7 to endosomes. We tested this hypothesis in yeast. *C. elegans* GFP-RAB-7 did not bind to membranes when expressed in yeast (Figure 5E). However, upon coexpression of SAND-1,

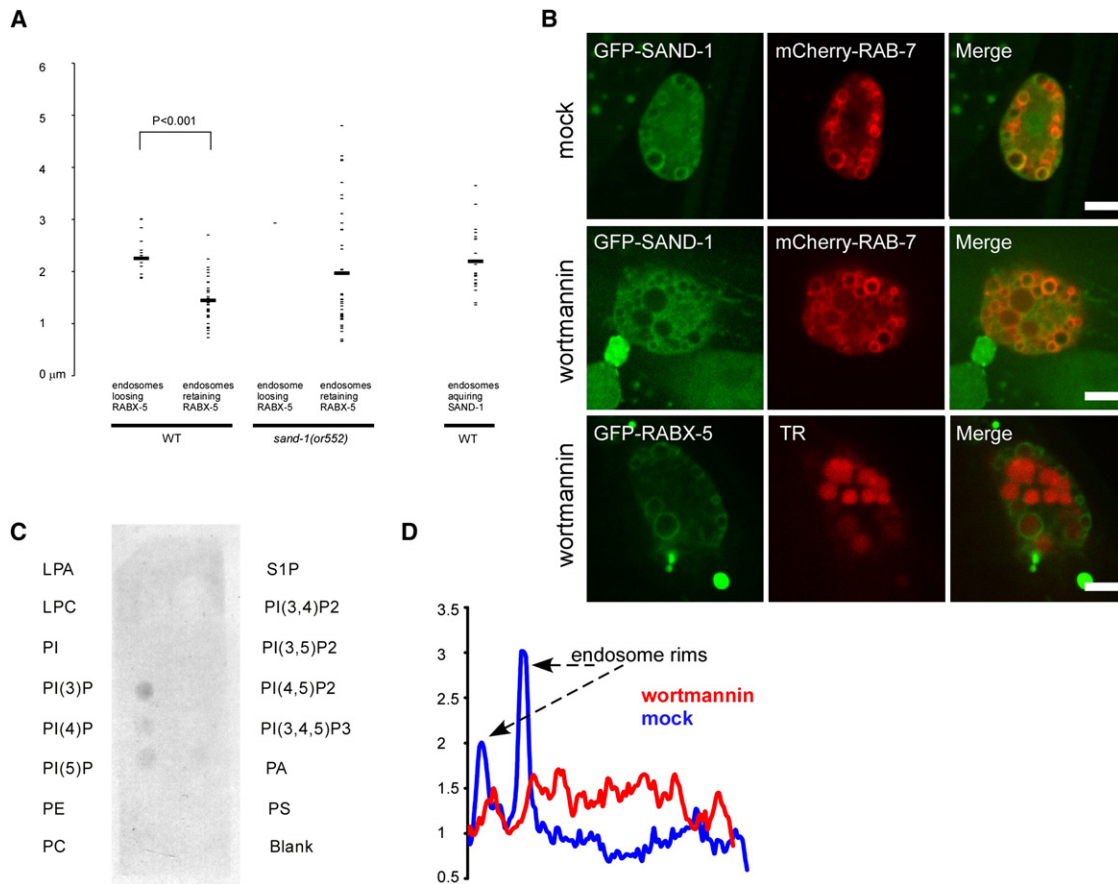


**Figure 6. Endosome Size and PI(3)P Levels May Drive Rab Conversion**

(A) RABX-5 is released from endosomes of a relative constant size. y-axis: diameter of the observed endosomes in  $\mu\text{m}$ . Total number of RABX-5-positive endosomes scored: wild-type, 51; *sand-1(or552)*, 41. Number of SAND-1-positive endosomes, 20.

(B) Wortmannin, injected into body cavity, abolished SAND-1 enrichment on endosomal membranes within 30 min after injection. RABX-5 and RAB-7 localization was not perturbed.

(C) Recombinant SAND-1 binds mono-phosphorylated phosphoinositides. The strongest signal is detected for PI(3)P.

(D) Typical line profile of the GFP::SAND-1 signal in mock- and wortmannin-treated coelomocytes.

See also Figure S5.

GFP-RAB-7 bound to the vacuole and the prevacuolar compartment, the yeast versions of the lysosome and the late endosome, respectively (Figure 5E). Therefore, SAND-1 plays an active role in the recruitment of RAB-7 to membranes.

#### SAND-1/Mon1b Interacts with the Core Components of the HOPS Complex

Because SAND-1/Mon1b and Rab7 did not interact directly (Poteryaev et al., 2007; Figure S2A), we asked whether SAND-1/Mon1 could interact with a member of the RAB-7 GEF complex, the HOPS complex. The HOPS complex is required for early-to-late endosome progression (Rink et al., 2005). SAND-1/Mon1b did not interact with the catalytic subunit of the HOPS complex Vps39 in a yeast two-hybrid assay (Figure 7D). However, we detected specific interaction between SAND-1/Mon1b and Vps18 and Vps11, both of which are core components of the Class C VPS/HOPS complex and are a part of the complex that is shared in yeast by HOPS and

CORVET (Peplowska et al., 2007; Figure 7D). The known interaction between SAND-1 and CCZ-1 (Poteryaev et al., 2007) served as a positive control. Moreover, recombinant HOPS complex members Vps16A, Vps18, Vps33A, and Vps41 bound to Mon1b-GST in vitro (Figure 7F), whereas the second SAND-1 homolog Mon1a only interacted with Vps33 in the in vitro pull down (Figure 7F), indicating that both proteins may have overlapping but not redundant functions. These interactions are specific because the Rabex5 interactor Rabaptin5 (Figure 7F), Rab5, and Rab7 (Figure S2) did not bind to Mon1b. Our results strongly suggest that SAND-1/Mon1 interacts with the core complex of the RAB-7 GEF to promote Rab7 activation on mature early endosomes to allow conversion to late endosomes. Taken together, our data demonstrate that SAND-1/Mon1 turns off RAB-5 activation and promotes RAB-7 activation via interaction with the respective GEFs and that SAND-1/Mon1 acts a sensor and switch for early-to-late endosome transition.

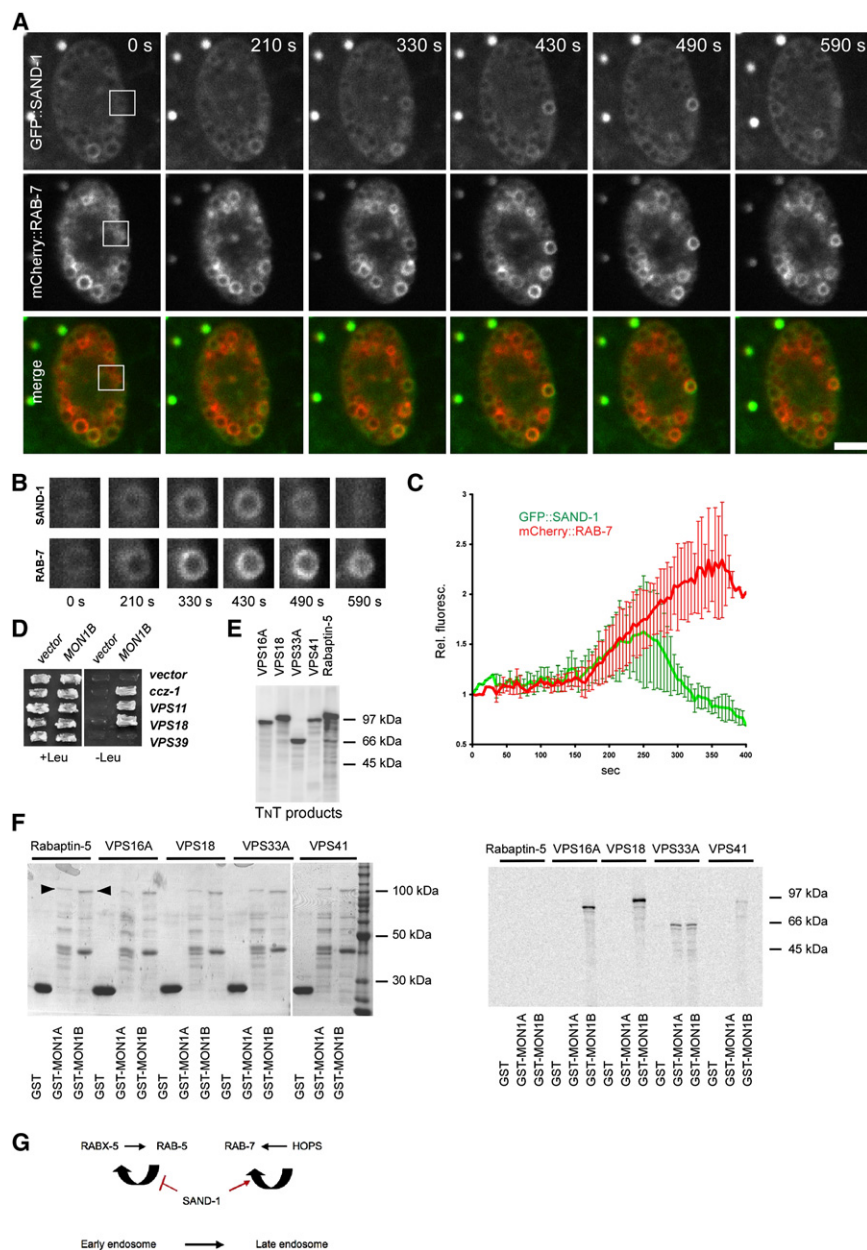


### Figure 7. SAND-1 and RAB-7 Arrive Concomitantly on Mature Early Endosomes

(A) The panel shows time frames of coelomocyte expressing GFP::SAND-1 and mCherry::RAB-7. One of the endosomes-in-transition is shown.

(B) Enlargement of the same endosome over time.

(C) Averaging of seven independent recordings of GFP::SAND-1 and mCherry::RAB-7 signals.

(D) Mon1a and Mon1b interact with HOPS complex members. Yeast two-hybrid interaction between Mon1b and Vps 11 and Vps18. The interaction with CCZ-1 serves as positive control.

(E) Autoradiograph of in vitro transcribed and translated HOPS complex members and Rabaptin-5 as a negative control. The translation reaction contained [<sup>35</sup>S] methionine and [<sup>35</sup>S] cysteine.

(F) The products of the transcription/translation reaction from (E) were used in a GST pull-down assay. The left panels represent Coomassie-stained gels indicating the amount of GST or GST-tagged proteins in the different assays. The arrowheads point to full-length GST-Mon1a and GST-Mon1b. The other bands correspond to degradation products. The autoradiograph of the GST pull-downs are shown in the right panel. Mon1a and Mon1b interact specifically with a subset of HOPS complex members but not with Rabaptin5.

(G) Model depicting the role of SAND-1/Mon1 in Rab conversion/early endosome maturation.

See also Movie S3.

The action of SAND-1 on RAB-5 and RAB-7 is conserved in different tissues in *C. elegans*, because RAB-5 and RAB-7 seemed to be regulated in a similar way in oocytes and the early embryo (Poteryaev et al., 2007). This conservation is not limited to *C. elegans* but extends to different species. We observed enlarged early endosomes in HeLa cells after knock down of the two mammalian isoforms, Mon1a and Mon1b. Therefore, SAND-1 function is conserved throughout metazoa.

Recently, a kinetic model was proposed (Del Conte-Zerial et al., 2008) in

which early-to-late endosome maturation is regulated by Rab GTPases through a cut-out switch. In this model, the levels of Rab5 would rise to a certain threshold and then suddenly drop. This drop of Rab5 levels would be brought about by the recruitment of Rab7. Therefore, Rab5 must also initiate a negative feedback loop, which will lead to its removal from the endosome. This negative feedback loop has two requirements: one would be to promote the recruitment of Rab7 onto endosomes, and the second would be to inhibit directly further activation of Rab5, for example, by either activating a Rab5-GAP or by inactivating or removing the Rab5-GEF from the maturing endosome, or both. SAND-1/Mon1 participates actively in both of these branches. The relative constant size with which early

## DISCUSSION

In this paper we demonstrate that Rab conversion is the molecular mechanism responsible for the transfer of proteins from early to late endosomes in *C. elegans* coelomocytes. Moreover, we show that SAND-1/Mon1 displaces RABX-5 from early endosomes, thereby interrupting the positive feedback loop of RAB-5 activation. Finally, SAND-1 is actively involved in the recruitment of RAB-7 to endosomes, probably through the recruitment or activation of Class C VPS/HOPS complex components to or on endosomes. Taken together, SAND-1 acts as a switch by turning off RAB-5 and turning on RAB-7 (Figure 7G). This switch then promotes the conversion from early to late endosomes.

endosomes undergo conversion would suggest that SAND-1 could recognize either a particular size or age of the endosome or the accumulation-specific factors. The age could be determined by the retrieval of other factors from early endosomes, similar to a distillation process, and only then conversion could occur. One of these accumulating determinants could be the PI(3)P. Determining the relative levels of PI(3)P using the 2xFYVE probe (Gillooly et al., 2000) fused to mRFP proved to be impossible. Unfortunately, the expression levels were very low and the signal-to-noise ratio too high to make any definitive statements (D.P. and A.S., unpublished results). The loss of RABX-5 from endosomes causes RAB-5 levels to drop as no new RAB-5 can be activated and recruited to early endosomes. Rebinding of RABX-5 to the endosomes might be prevented by monoubiquitination of RABX-5. Mattera and Bonifacino (2008) showed that monoubiquitinated Rabex-5 is enriched in the cytoplasm. Concomitantly with SAND-1, Rab7 arrives at the maturing endosome and is activated there by the Rab7-GEF complex, the Class C VPS/HOPS complex. The Class C VPS/HOPS complex has been shown to be present on maturing endosomes and can interact with Rab5-GTP (Rink et al., 2005). We found that the mammalian SAND-1/Mon1b interacts with five members of the Class C VPS/HOPS complex—Vps11, Vps16A, Vps18, Vps33, and Vps41—but not with the catalytic subunit Vps39. Thus, Rab5 could drive the recruitment of the downstream-acting Rab, Rab7. This scenario is strikingly similar to the coupling of the activation of Ypt31/32 and Sec4 (Ortiz et al., 2002). Vps11, Vps16A, Vps18, and Vps33 are also part of the CORVET complex in yeast (Peplowska et al., 2007), which also binds to yeast Rab5, Ypt51a/Vps21, and can be converted into a HOPS complex. Given the conservation of the early steps of endocytosis from yeast to mammals, it seems likely that the CORVET complex also exists in *C. elegans* and in mammalian cells. Thus, alternatively, SAND-1 may drive the conversion of the CORVET complex into the HOPS complex and thereby activate the GEF for Rab7. Consistently with a function of VPS-18 and VPS-11 on early endosomes, endosome biogenesis is altered in a *vps-18* mutant (Xiao et al., 2009), yet no large early endosomes accumulated. Therefore, it seems unlikely that the Class C VPS/HOPS complex alone would be driving Rab conversion and endosome maturation, as predicted by the model (Del Conte-Zerial et al., 2008). It is improbable that SAND-1 could act as RabGEF for Rab7 itself because Rab7 levels on endosomes continued to rise, when SAND-1 levels have already dropped (Figure 6), and Mon1b could not bind Rab7-GDP (Figure S2A). Our data are more consistent with SAND-1 acting as a switch by controlling the action of 2 RabGEFs; it negatively regulates RABX-5 by displacing it from the membrane and it positively drives the activation of the HOPS complex.

In yeast, Mon1p is found in complex with Ccz1p, and they are thought to function in a complex (Wang et al., 2002). Because this interaction between SAND-1 and CCZ-1 is conserved in *C. elegans* (Poteryaev et al., 2007; Poteryaev and Spang, 2005), it seems likely that CCZ-1 is also involved in early-to-late endosome conversion.

The observed endosomal maturation is mechanistically related to the transport through the Golgi apparatus, which is currently assumed to function by Golgi maturation (Losev

et al., 2006; Matsuura-Tokita et al., 2006). In both processes, proteins are sorted away from the compartment that matures. COPI-coated vesicles bud off the rim of the cisternae and travel in retrograde direction to fuse with a cisterna that is oriented more toward the *cis*-side of the Golgi apparatus (Allan and Balch, 1999). In the case of early-to-late endosome maturation, proteins are sorted away through at least three different pathways: through recycling endosomes (de Renzis et al., 2002; de Wit et al., 2001; Peden et al., 2004) and through two distinct pathways to the TGN, one epsinR and Rab6-dependent and the other one the involving the retromer complex (Bonifacino and Hurley, 2008; Saint-Pol et al., 2004; Seaman et al., 1998). Hence, transport through the endosomal system and through the Golgi apparatus could employ similar mechanisms.

## EXPERIMENTAL PROCEDURES

### Yeast Methods

*C. elegans* cDNAs were amplified from a plasmid library (H. Doi and A. Terasaki, RIKEN Bioresource Center, Japan). To generate plasmids carrying GFP-tagged *C. elegans rabx-5*, full-length and truncated cDNA of *rabx-5* were inserted into XhoI site of pUG34 plasmid (gift from J. H. Hegemann). The resulting construct is the N-terminal GFP fusion under control of methionine-repressible *MET25* promoter. *rab-5* and *rab-7* were cloned into the same vector using EcoRI and XhoI sites. For coexpression of *C. elegans sand-1*, the following vectors were used: *sand-1* cDNA was cloned into p426GPD and p416GPD for constitutive expression and into p426ADH and p416ADH for controlled expression (Mumberg et al., 1995). To express the truncated *sand-1*, p426GPD-*sand-1* plasmid was digested with ClaI and XhoI, and the termini were filled by treatment with Klenow enzyme and self-ligated. The plasmids were transformed into yeast strain BY4741 (*Mat a*; *his3Δ1*; *leu2Δ0*; *met15Δ0*; *ura3Δ0*). Yeast two-hybrid experiments were performed with the LexA system (Golemis and Khazak, 1997). Human *MON1A*, *MON1B*, *VPS11*, *VPS16*, *VPS18*, *VPS33*, *VPS39*, and *VPS41* full-length cDNA clones were purchased from OriGene Technologies (Rockville, MD). Full-length cDNAs of *sand-1* or *MON1B* was used as bait in the pEG202 vector. To test the interaction with candidate genes, the cDNAs were cloned into the pJG4-5 prey vector. The bait and prey plasmids were cotransformed into the EGY48 reporter strain. To assess the expression of the *LEU2* reporter, transformants were grown on plates that lack histidine, tryptophan and leucine for 2 days at 30°C.

### *C. elegans* Methods and Strains

*C. elegans* strains were derived from the wild-type Bristol strain N2. Worm cultures, genetic crosses, and other *C. elegans* methods were performed according to standard protocols (Brenner, 1974). Wild-type and *sand-1(or552)* strains and their transgenic derivatives were grown at 20°C, which is a semipermissive temperature for *or552* allele. At this temperature, the endosomal trafficking defects are as severe as at 25°C, but most of the worms are viable (Poteryaev et al., 2007). The following previously created transgenic strains were used: RAB-5-GFP *sand-1+* strain NP212 *cdEx49[Pcc1::GFP::RAB-5, Pmyo-2::GFP]*, RAB-5-GFP, and *sand-1(or552)* strain FA71 *sand-1(or552); cdEx49[Pcc1::GFP::RAB-5, Pmyo-2::GFP]*.

### Cell Culture and RNA Interference

HeLa cells expressing GFP-tagged Rab5c under the endogenous promoter (Poser et al., 2008) were cultured at 37°C and 5% CO<sub>2</sub> in Dulbecco's modified Eagle's medium (DMEM) supplemented with 10% fetal calf serum, 2 mM L-glutamine, 100 U/ml penicillin, and 100 μg/ml streptomycin.

RNA interference was performed in a 24-well plate for imaging or in a six-well plate for quantitative real time PCR. Three individual Stealth Select RNAi siRNA duplexes (Invitrogen) were used for each of *mon1A* and *mon1B*. Cells were transfected with 5 nM of siRNA using interferin™ transfection reagent (polyplus siRNA transfection reagent). In case of double knockdown experiments,

different combinations of mon1A and mon1B siRNA duplexes were used keeping individual siRNA concentration at 5 nM. The extent of knockdown was quantified by RT-PCR on total RNA extracted using RNeasy spin-columns (QIAGEN, Hilden Germany), transcribed with Superscript III reverse transcriptase (Invitrogen, Karlsruhe, Germany) and oligo-dT primers, quantified in Cybr-Green RT-PCRs (Stratagene, La Jolla, CA) using 5' ACTCTTCACC AGCCCTGAG, 3' AGGAAGCAGAGTCCAAGCTG primers for mon1A and 5' GAGGAAACAGGATCCAAGG, 3' CCGAGAGGTGCTTTGACAG for mon1B, keeping annealing temperature at 58°C. For the estimation of the knockdown effect by immunoblot, cells transfected with different siRNAs were lysed 72 hr after transfection. Cells were lysed with cell lysis buffer (25 mM Tris-HCl [pH 7.2], 100 mM NaCl, 1% Triton X-100, 1 mM EDTA, 1 mM DTT, 1 mM PMSF, and 1 mg/ml each of aprotinin and leupeptin). Cell lysates were analyzed by immunoblot using antibodies against Mon1a and Mon1b, respectively. For Mon1b knockdown, the intensities of the bands were normalized with respect to that of the mock transfection. The experiment was repeated three times, and the results were plotted as a bar graph.

#### Endosome Recruitment Assay

The endosomes were purified from HeLa cells by use of a sucrose sedimentation method (Gorvel et al., 1991). The purified endosomes were incubated with 15 nM Rabex5-Rabaptin5 and 10 nM Rab5-GDI for 25 min at 37°C with gentle shaking (300 rpm). The reaction was stopped by transferring the reaction tubes on ice. The reaction mixture was subsequently subjected to Histodenz step-gradient centrifugation in order to separate the endosomal fraction from the soluble proteins and disrupted membranes. The second fraction from the top, which is enriched in endosomes, was split and incubated either in the presence or absence of 30 nM Mon1b at 37°C under gentle agitation. Endosomes were reisolated over a Histodenz step-gradient, as described above. Fractions collected from the top were separated by SDS PAGE. The amount of Rabex5 and Rab5 in the different fractions was assessed by immunoblot using  $\alpha$ -Rabex5 and  $\alpha$ -Rab5 antibodies.

#### Microscopy and Trafficking Experiments in Coelomocytes

Live worms, immobilized with 20 mM levamisole in M9 were mounted on agarose pads cast on microscopy slides. The worms were imaged with a spinning disk confocal system Andor Revolution (Andor Technologies, Belfast, Northern Ireland) mounted onto an IX-81 inverted microscope (Olympus, Center Valley, PA), equipped with iXon<sup>EM</sup>+ EMCCD camera (Andor Technologies). Specimens were imaged using a 60 $\times$  1.42 N.A. oil objective. Each pixel represents 0.107  $\mu$ m. Excitation was achieved using solid-state 488 nm and 560 nm lasers. Exposure times were between 0.1 and 0.2 s. Each image was a result of four averaged frames. For 4D microscopy, the typical number of planes in the Z direction was five. Each Z-step was normally 0.5  $\mu$ m. The images were exported as TIFF files and occasionally adjusted for contrast in Image J. No nonlinear adjustments were used. Endosomes were manually tracked using image J. The acceptance criteria for the endosome, which we took into account was that, in a given 4D space, we could unambiguously track it manually. For the fluorescence intensity measurements, we drew a contour, which included the rim of an endosome, and measured the mean gray value within this contour. If the endosome drifted away along the Z-axis, we would switch to the neighboring Z plane to locate the largest endosome diameter. In many cases, however, the tracking was done within one Z plane, because there was sufficient number of endosomes staying within tracking parameters.

The traffic of BSA-TR in coelomocytes was monitored as described previously (Zhang et al., 2001). For wortmannin treatment, adult worms were injected with either 0.1% DMSO or 1  $\mu$ M wortmannin in 0.1% DMSO. After the recovery on seeded NGM plates for 30–40 min, the worms were mounted on agar pads for live microscopy.

#### Immunofluorescence Microscopy and Image Analysis of Tissue Culture Cells

Cells ( $n = 15,000$ ) were plated per well in 24-well plate. A reverse transfection protocol was used in which siRNA and interferin<sup>TM</sup> reagent were mixed inside the wells and the cells were overlaid subsequently. Seventy-two hours after transfection, cells were either fixed with 4% paraformaldehyde/PBS or rinsed with serum-free medium and were incubated in the same containing 50 nM

Dil-LDL before fixation. The fixed cells were mounted on a glass slide and imaged using a Zeiss LSM duoscan microscope (63 $\times$  oil, 1.4, 1 Airy unit). Data from three independent experiments were subjected to data analysis by the automated image analysis program, MotionTracking (Rink et al., 2005). Fifty images per condition were analyzed, which represented 200 cells and about 35,000 GFP-Rab5 vesicles. The area of each GFP-positive punctate structure was calculated, and cumulative distributions of areas were plotted for control and knockdown conditions. The significance of the difference between a given pair of distributions was performed using a Z-test.

#### GST Pull-Down of VPS-C Proteins

TNT T7 Quick Coupled Transcription/Translation System (Promega, WI) was used to produce [<sup>35</sup>S]-labeled VPS-C proteins. Full-length cDNA clones of VPS-C genes (OriGene Technologies, MD) were used as templates for transcription. Up to 100  $\mu$ g of GST fusion proteins (Mon1a-GST, Mon1b-GST, or GST) were immobilized onto GSH-sepharose beads. The unbound proteins were removed, and the in vitro-translated proteins were added to the immobilized GST fusion proteins. After incubation at 4°C for 2 hr in 20 mM HEPES (pH 7.5), 150 mM NaCl, 0.5 mM EDTA, 10% glycerol, 0.5% Triton X-100, and 1 mM DTT, the beads were washed five times. The bound VPS proteins were resolved on SDS PAGE and visualized using a PhosphorImager (GE Healthcare, Freiburg, Germany).

#### SUPPLEMENTAL INFORMATION

Supplemental Information includes Extended Experimental Procedures, five figures, and three movies and can be found with this article online at doi:10.1016/j.cell.2010.03.011.

#### ACKNOWLEDGMENTS

We thank H. Fares, N. Andrews, and J. Hegemann for reagents and I.G. Macara and M. Labouesse for critical reading of the manuscript. L. Bermudo and I.G. Macara are acknowledged for fruitful discussions, and B. Grant is thanked for providing information about the RABX-5 ORF. This work was supported by the University Basel, the Swiss National Science Foundation (A.S.), and the Max Planck Society (M.Z.).

Received: July 30, 2009

Revised: November 26, 2009

Accepted: February 25, 2010

Published: April 29, 2010

#### REFERENCES

- Allan, B.B., and Balch, W.E. (1999). Protein sorting by directed maturation of Golgi compartments. *Science* 285, 63–66.
- Bonifacino, J.S., and Hurley, J.H. (2008). Retromer. *Curr. Opin. Cell Biol.* 20, 427–436.
- Brenner, S. (1974). The genetics of *Caenorhabditis elegans*. *Genetics* 77, 71–94.
- Christoforidis, S., McBride, H.M., Burgoyne, R.D., and Zerial, M. (1999). The Rab5 effector EEA1 is a core component of endosome docking. *Nature* 397, 621–625.
- de Renzis, S., Sonnichsen, B., and Zerial, M. (2002). Divalent Rab effectors regulate the sub-compartmental organization and sorting of early endosomes. *Nat. Cell Biol.* 4, 124–133.
- de Wit, H., Lichtenstein, Y., Kelly, R.B., Geuze, H.J., Klumperman, J., and van der Sluijs, P. (2001). Rab4 regulates formation of synaptic-like microvesicles from early endosomes in PC12 cells. *Mol. Biol. Cell* 12, 3703–3715.
- Del Conte-Zerial, P., Bruschi, L., Rink, J.C., Collinet, C., Kalaidzidis, Y., Zerial, M., and Deutsch, A. (2008). Membrane identity and GTPase cascades regulated by toggle and cut-out switches. *Mol. Syst. Biol.* 4, 206.

- Delprato, A., Merithew, E., and Lambright, D.G. (2004). Structure, exchange determinants, and family-wide rab specificity of the tandem helical bundle and Vps9 domains of Rabex-5. *Cell* *118*, 607–617.
- Gerrard, S.R., Bryant, N.J., and Stevens, T.H. (2000). VPS21 controls entry of endocytosed and biosynthetic proteins into the yeast prevacuolar compartment. *Mol. Biol. Cell* *11*, 613–626.
- Gillooly, D.J., Morrow, I.C., Lindsay, M., Gould, R., Bryant, N.J., Gaullier, J.M., Parton, R.G., and Stenmark, H. (2000). Localization of phosphatidylinositol 3-phosphate in yeast and mammalian cells. *EMBO J.* *19*, 4577–4588.
- Golemis, E.A., and Khazak, V. (1997). Alternative yeast two-hybrid systems: the interaction trap and interaction mating. *Methods Mol. Biol.* *63*, 197–218.
- Gorvel, J.P., Chavrier, P., Zerial, M., and Gruenberg, J. (1991). rab5 controls early endosome fusion in vitro. *Cell* *64*, 915–925.
- Losev, E., Reinke, C.A., Jellen, J., Strongin, D.E., Bevis, B.J., and Glick, B.S. (2006). Golgi maturation visualized in living yeast. *Nature* *441*, 1002–1006.
- Matsuura-Tokita, K., Takeuchi, M., Ichihara, A., Mikuriya, K., and Nakano, A. (2006). Live imaging of yeast Golgi cisternal maturation. *Nature* *441*, 1007–1010.
- Mattera, R., and Bonifacino, J.S. (2008). Ubiquitin binding and conjugation regulate the recruitment of Rabex-5 to early endosomes. *EMBO J.* *27*, 2484–2494.
- Mumberg, D., Muller, R., and Funk, M. (1995). Yeast vectors for the controlled expression of heterologous proteins in different genetic backgrounds. *Gene* *156*, 119–122.
- Ortiz, D., Medkova, M., Walch-Solimena, C., and Novick, P. (2002). Ypt32 recruits the Sec4p guanine nucleotide exchange factor, Sec2p, to secretory vesicles; evidence for a Rab cascade in yeast. *J. Cell Biol.* *157*, 1005–1015.
- Peden, A.A., Schonteich, E., Chun, J., Junutula, J.R., Scheller, R.H., and Prekeris, R. (2004). The RCP-Rab11 complex regulates endocytic protein sorting. *Mol. Biol. Cell* *15*, 3530–3541.
- Peplowska, K., Markgraf, D.F., Ostrowicz, C.W., Bange, G., and Ungermann, C. (2007). The CORVET tethering complex interacts with the yeast Rab5 homolog Vps21 and is involved in endo-lysosomal biogenesis. *Dev. Cell* *12*, 739–750.
- Poser, I., Sarov, M., Hutchins, J.R., Heriche, J.K., Toyoda, Y., Pozniakovsky, A., Weigl, D., Nitzsche, A., Hegemann, B., Bird, A.W., et al. (2008). BAC TransgeneOmics: a high-throughput method for exploration of protein function in mammals. *Nat. Methods* *5*, 409–415.
- Poteryaev, D., Fares, H., Bowerman, B., and Spang, A. (2007). *Caenorhabditis elegans* SAND-1 is essential for RAB-7 function in endosomal traffic. *Embo. J.* *26*, 301–312.
- Poteryaev, D., and Spang, A. (2005). A role of SAND-family proteins in endocytosis. *Biochem. Soc. Trans.* *33*, 606–608.
- Rink, J., Ghigo, E., Kalaidzidis, Y., and Zerial, M. (2005). Rab conversion as a mechanism of progression from early to late endosomes. *Cell* *122*, 735–749.
- Rosenfeld, J.L., Moore, R.H., Zimmer, K.P., Alpizar-Foster, E., Dai, W., Zarka, M.N., and Knoll, B.J. (2001). Lysosome proteins are redistributed during expression of a GTP-hydrolysis-defective rab5a. *J. Cell Sci.* *114*, 4499–4508.
- Saint-Pol, A., Yelamos, B., Amessou, M., Mills, I.G., Dugast, M., Tenza, D., Schu, P., Antony, C., McMahon, H.T., Lamaze, C., et al. (2004). Clathrin adaptor epsinR is required for retrograde sorting on early endosomal membranes. *Dev. Cell* *6*, 525–538.
- Sato, M., Sato, K., Fonarev, P., Huang, C.J., Liou, W., and Grant, B.D. (2005). *Caenorhabditis elegans* RME-6 is a novel regulator of RAB-5 at the clathrin-coated pit. *Nat. Cell Biol.* *7*, 559–569.
- Seachrist, J.L., Anborgh, P.H., and Ferguson, S.S. (2000). beta 2-adrenergic receptor internalization, endosomal sorting, and plasma membrane recycling are regulated by rab GTPases. *J. Biol. Chem.* *275*, 27221–27228.
- Seaman, M.N., McCaffery, J.M., and Emr, S.D. (1998). A membrane coat complex essential for endosome-to-Golgi retrograde transport in yeast. *J. Cell Biol.* *142*, 665–681.
- Shin, H.W., Hayashi, M., Christoforidis, S., Lacas-Gervais, S., Hoepfner, S., Wenk, M.R., Modregger, J., Uttenweiler-Joseph, S., Wilm, M., Nystuen, A., et al. (2005). An enzymatic cascade of Rab5 effectors regulates phosphoinositide turnover in the endocytic pathway. *J. Cell Biol.* *170*, 607–618.
- Spang, A. (2009). On the fate of early endosomes. *Biol. Chem.* *390*, 753–759.
- Stenmark, H., Valencia, A., Martinez, O., Ullrich, O., Goud, B., and Zerial, M. (1994). Distinct structural elements of rab5 define its functional specificity. *EMBO J.* *13*, 575–583.
- Vonderheit, A., and Helenius, A. (2005). Rab7 associates with early endosomes to mediate sorting and transport of Semliki forest virus to late endosomes. *PLoS Biol.* *3*, e233.
- Wang, C.W., Stromhaug, P.E., Shima, J., and Klionsky, D.J. (2002). The Ccz1-Mon1 protein complex is required for the late step of multiple vacuole delivery pathways. *J. Biol. Chem.* *277*, 47917–47927.
- Xiao, H., Chen, D., Fang, Z., Xu, J., Sun, X., Song, S., Liu, J., and Yang, C. (2009). Lysosome biogenesis mediated by vps-18 affects apoptotic cell degradation in *Caenorhabditis elegans*. *Mol. Biol. Cell* *20*, 21–32.
- Zhang, Y., Grant, B., and Hirsh, D. (2001). RME-8, a conserved J-domain protein, is required for endocytosis in *Caenorhabditis elegans*. *Mol. Biol. Cell* *12*, 2011–2021.
- Zhu, H., Zhu, G., Liu, J., Liang, Z., Zhang, X.C., and Li, G. (2007). Rabaptin-5-independent membrane targeting and Rab5 activation by Rabex-5 in the cell. *Mol. Biol. Cell* *18*, 4119–4128.